Journal of Drug Delivery Science and Technology xxx (xxxx) xxx

Contents lists available at ScienceDirect

Journal of Drug Delivery Science and Technology

journal homepage: www.elsevier.com/locate/jddst

Development and characterization of 5-fluorouracil nanofibrous film for the treatment of stomach cancer

Pooja Anothra [a], Deepak Pradhan [b], Pradeep Kumar Naik [c], Goutam Ghosh [b], Goutam Rath [b,*]

[a] Department of Pharmaceutics, I.S.F.College of Pharmacy, Moga, Punjab, India
[b] School of Pharmaceutical Sciences, Siksha 'O' Anusandhan (Deemed to Be University), Odisha, India
[c] Department of Biotechnology & Bioinformatics. Sambalpur University, Odisha, India

ARTICLE INFO

Keywords:
Nanofibers
5-Fluorouracil
Eudragit S-100
Gastroretentive
Gastric cancer

ABSTRACT

The purpose of the present exposition was to develop 5-fluorouracil (5-FU) loaded gastro retentive nanofibrous film, to improve the chemotherapeutic performance in gastric cancer. 5-FU loaded Eudragit S-100 composite nanofibers have been prepared and optimized using a single nozzle electrospinning technique. The prepared nanofibers were evaluated for inclusive pharmaceutical aspects including drug encapsulation, physical properties, surface morphology, buoyancy, tensile strength, thermal properties, and *in-vitro* release. The developed formulation shows high % drug encapsulation (>90%), superior thermal stability, and released 90% of encapsulated therapeutic after 12 h. The optimized formulation was subjected to *in-vivo* antitumor performance against Ehrlich Ascites Carcinoma (EAC) induced orthotopic xenograft models. The developed nanofiber formulation exhibits superior tumor regression potential and pharmacokinetic profile compared to the plain drug. Experimental findings suggest that a nanofiber-based gastro retentive drug delivery system offers a potential strategy for the localized treatment of gastric cancer with improved chemotherapeutic performance.

1. Introduction

Gastric cancer is the third leading cause of cancer-related deaths in the world, and approx. half of all cases occur in eastern Asia [1]. The prevalence of gastric cancer is also high in countries like Russia, Costa Rica, and South America. According to GLOBOCAN 2012, stomach cancer is the fifth (1.0 million cases, 5.7%) leading cause of cancer-related deaths globally. Further, unusual dietary habits, stressful lifestyle, tobacco, and alcohol increases the risk of gastric cancer. In Korea, a screening program was performed for early detection of gastric cancer among high-risk groups in 1999 results better clinical outcomes with a significant decrease in the mortality rate related to gastric cancer [2].

However, advanced gastric cancer with gastric outlet obstruction (GOO) is found in a considerable number of patients with a very low survival rate as short as 3–4months [3]. Treatments of stomach cancer usually include chemotherapy, radiation, surgery, immunotherapy, or often combination of one or more treatment approach based on the conditions. Currently, chemotherapy remains the valid therapeutic options used for the treatment of stomach cancer. Conventional oral chemotherapy used to treat gastric cancer suffer from major constraints like low bioavailability, multiple dosing, and systemic toxicity leads to poor treatment outcomes. Low or variable bioavailability of oral chemotherapy is often associated with low drug solubility, premature drug release, and short retention time [4]. Gastric bioavailability of oral chemotherapeutics is largely determined by the drug characteristics and nature of the dosage form. Gastro retentive drug delivery system (GRDDS) is particularly suitable to combat challenges related to pharmacokinetic barriers associated with oral chemotherapy [5]. GRDDS due to its prolonged gastric retention time and modulated drug release input helps in achieving targeted drug release over an extended period [6]. Further, these systems are useful to enhance the therapeutic efficacy of chemotherapeutics which have a narrow absorption window like 5-FU. GRDDS have been extensively investigated for the last two decades and are a topic of interest in terms of their potential for the controlled drug delivery at the targeted site. The controlled gastric retention of solid dosage forms may be achieved by the mechanism of mucoadhesion, floatation, expansion, or by the simultaneous administration of pharmacological agents that delay gastric emptying. However, the selection of appropriate polymer and dosage form design is important to meet the therapeutic goal. Nanofiber can be a good choice for the gastro retentive drug delivery system. Nanofibers because of their high

* Corresponding author. Department of Pharmaceutics, India.
E-mail address: goutamrath123@gmail.com (G. Rath).

https://doi.org/10.1016/j.jddst.2020.102219
Received 27 May 2020; Received in revised form 6 October 2020; Accepted 11 November 2020
Available online 20 November 2020
1773-2247/

surface area to volume ratio and high pore volume, generate ultra-low-density materials appropriate for floating drug delivery systems [7]. It can be designed into a matrix or reservoir system and can be incorporate a wide range of pharmaceuticals. In our previous study, we have observed polylactic acid nanofiber-based GRDDS release approx. 60% of drugs (Diacerein) after 30 h in simulated gastric fluid [8]. In another study we have found PVA nanofibers with a diameter ranging from 150 to 180 nm, releases about 90% of drug (Fluconazole) in about 6–8 h. Therefore, an appropriate selection of polymer and drug perhaps contributing to the most important role to achieve the desired therapeutic outcome of the drug in nanofibers [9]. 5-FU has been extensively used in clinical practice for the treatment of gastric carcinoma. Moreover, the physicochemical properties of 5-FU including pKa (8.0), molecular weight (130.08 g/mol), solubility (2–5 mg/mL), potency (0.83 mg/kg) and superior stability of the drug in gastric pH, makes it a suitable drug candidate for gastro retentive drug delivery system. However, poor aqueous solubility and short half-life (10–12 min) need to be overcome. Therefore, drug carriers with intrinsic ability to enhance drug solubility and modulate release kinetics may be employed to deal with the above issues. Electrospinning allows instant solidification of liquid jet causes phase transition of some drugs resulting in an enhancement in aqueous solubility of drugs. In our earlier study, we have observed a 3-fold increase in aqueous solubility of diacerein in nanofiber formulation compared to a native drug [8]. Eudragit S-100 is a biocompatible polymer, extensively studied in oral controlled drug delivery application. Eudragit S-100 because of its polyanionic nature, exhibit controlled swelling in gastric environment allow custom-tailored release of encapsulated drug. Eudragit remains deprotonated at gastric pH and thus prevent a sudden onset of drug release. Eudragit S-100 is not soluble in water and acidic pH and it is also considered as food grade polymer because of its non-toxic nature [9,10]. According to the literature evidence, eudragit microparticles in gastric medium showed a better protection of encapsulated drug [11]. Looking at the solubility trend of Eudragit S-100 and 5-FU in ethanol, the present study attempts on the above composition to improve the loading capacity. Further, in the present application, methylcellulose is used as a mucosal protectant to reduce mucosal toxic consequences occurs as a result of chemotherapy [12]. Methyl cellulose due to the presence of polyfunctional carboxylic acids is extensively used as synthetic mucoadhesive polymer in gastroretentive drug delivery [13,14]. Moreover, both Eudragit S-100 and methylcellulose approved by USFDA as safe and nonimmunogenic for human use and has no specified limitations regarding use. In addition to above the proposed carrier incorporated with a radiocontrast material such as barium sulfate, thus provide an opportunity to guide chemotherapeutic utility based on cancer physiology. Further barium sulfate allows determining the targeting potential of the proposed carrier. The proposed hypothesis opens a new avenue for real-time controlled and localized delivery of chemotherapeutics according to the physiological requirement of tumors.

2. Materials and methods

2.1. Materials

5-FU was obtained as a gift sample from United Biotech Pvt. Ltd., H. P. India. Eudragit S-100 procured from Evonik. India. Ehrlich Ascites Carcinoma cell lines were purchased from NCCS, Pune, India. Methylcellulose and barium sulfate were purchased from Merck, India. RPMI 1640 media supplemented with 10% heat-inactivated FBS for mammalian cells was procured from Hi-Media Laboratories, India. All other chemicals used are of analytical grade.

2.2. Preparation of eudragit S-100 nanofibers

In this method, the required quantity of polymers (Eudragit S-100 and Methylcellulose) were dissolved in a solvent mixture (about 90% ethanol and 10% water) to produce concentrations of 15% and 0.05% w/v towards Eudragit S-100 and Methylcellulose respectively. The mixture was stirred continuously for 10 h at ambient conditions to obtain a clear homogenous dispersion. After 10 h of mixing, the final volume was made with the above solvent mixture to maintain the concentrations at 15% and 0.05% respectively for Eudragit S-100 and methylcellulose. The core polymer solution was then transferred to a 5 ml syringe attached with a 25-gauge metal needle. The syringe with the polymer solution was then connected to the infusion pump operate at a controlled feed rate of 0.1–0.5 ml/h. Electrospinning was performed under different process conditions (Applied potential (15-20 KV), Tip to collector distance (10–15 cm) to identify optimal process parameters to produce nanofibers with desired properties. Nanofibers were collected on a flat collector plate, placed opposite to winged needle set. The nanofibers were dried at room temperature and stored under optimum condition until further analysis.

2.3. Preparation of drug-loaded nanofibers

In the present study, a passive loading technique was adopted to prepare drug-loaded nanofibers (Rath et al., 2016). A saturated solution of 5-FU in 10 mL of the above polymer combination was prepared at room temperature as per the method described earlier. The drug-polymer mixture was stirred continuously for 12 h at room conditions to obtain a clear homogenous dispersion. The drug-polymer solution was then placed to a 5 ml syringe attached with a 25gauge metal needle. The syringe with the polymer solution was then connected to the infusion pump operate at a controlled feed rate of 0.1–0.5 ml/h. The electrospinning of the prepared mixture was performed under predefined spinning parameters to fabricate drug-loaded nanofibers with desired properties. The developed nanofibers were dried at room temperature and stored under optimum condition until further analysis.

2.4. Characterization of nanofibers

The prepared nanofibers (blank and drug-loaded) were analyzed for surface morphology using scanning electron microscopy (FE-SEM, Nova nano India). Morphological analysis of nanofibers was performed to analyze the changes in fiber diameter and surface topography before and after the incorporation of the drug. Briefly, the blank and drug-loaded nanofiber of area 1 cm^2 was transferred to the sample holder and coated with platinum for 10 min. The samples were then subjected to SEM analysis at a voltage of 15kv. IR studies were executed to identify the possible interaction between drug and polymer in the finished formulation. Briefly, 1 mg of prepared sample was mixed with 100 mg of IR grade KBr and then the mixture was compressed using a hydraulic press (10000 psi) to form pellets. KBr pellets being formed were scanned at the wavenumber range (400–4000 cm^{-1}). The apparent density and porosity of electrospun fibrous mats were calculated using the following formula;

$$Apparent = (g\ cm3) = \frac{Mat\ mass\ in\ g}{mat\ thickness(g)*mat\ area(cm2)}$$

$$mat\ porosity = 1 - \frac{Mat\ apparent\ density\ (gcm3)}{Bulk\ density\ of\ Eudragit\ S-100}*100\%$$

Purity profile and possible physical transformation of the drug in the developed formulation were analyzed by both DSC and XRD. DSC measurements were performed in a perforated aluminum pan containing the sample, heating at a rate of 5°C/min from 30 to 300°C. Similarly, the changes in the crystallinity of drugs in the finished formulation were analyzed by an X-ray diffractometer. The prepared samples were subjected to monochromatic radiation (45 kV, 40 mA) using a wide-angle X-ray diffractometer with a scanned angle from 5° to 70°.

2.4.1. In-vitro drug release

In-vitro release of the plain drug (control sample), loaded nanofibers were determined at 37 °C in a simulated gastric fluid (pH 1.2) in a shaking incubator. Sampling was done at predefined time intervals after 1, 2, 3, 4, 5, 6, 8, 10, and 12 h. The volume of samples withdrawn for drug analysis was adjusted with an equal volume of fresh simulated gastric fluid to maintain sink conditions. The amount of drug was determined using a UV–Vis spectrophotometer at λ_{max} of 265 nm. The drug release data of 5-FU loaded nanofibers was fitted to different mathematical models (Higuchi's, zero-order, and first-order) to understand their release mechanisms. The data were analyzed using MS Excel statistical function. The model for drug release study was selected based on the highest correlation coefficient (r^2) value.

2.5. Encapsulation efficiency

The encapsulation efficiency (EE) of the developed formulation was determined using the following formula. Encapsulation efficiency was determined in triplicate by dissolving 76.25 mg of prepared nanofibers in ethanol and the amount of drug was determined by using UV–Visible Spectroscopy at the selected wavelength (265 nm). The EE was calculated by the formula:

$$Encapsulation\ Efficiency(\%) = \frac{Amount\ of\ drug\ in\ nanofibers}{Drug\ initially\ added} \times 100$$

2.5.1. Tensile strength

Mechanical strength of the prepared formulation (blank nanofiber and drug-loaded nanofiber) was determined by a Brookfield CT3 texture analyser. Prepared film of size 5 × 2 cm^2 was placed in a vertical axial position using clamps. The device was run after an initial adjustment at a load of 1 kg. The tensile force which was necessary to split the fiber was determined [15].

2.5.2. Mucoadhesion strength

The force required for the complete separation of nanofiber film from goat mucosa is quantified with the help of Brookfield CT3 texture analyser. Firstly, the pre-treated goat mucosa was fixed to one of the attachments of the instrument and a prepared film of 2 cm^2 diameter was stuck to the complimentary attachment using double-sided self-adhesive tape. Both the sides were made in contact by applying 1 kg/cm^2 pressure for 15s [15]. The force required for complete detachment of fibers from the mucosa was determined from the strip chart.

2.5.3. Degradation of polymer

In-vitro degradation of developed nanofiber film was measured using the gravimetric method. Developed nanofiber film of 2 cm^2 area was transferred into a 1000 mL beaker containing 900 mL simulated gastric fluid (SGF). After a predefined period, the remaining sample was recovered from the medium and dried in vacuum at room temperature until the weight is constant for two successive readings. The weight of the film was determined using a digital balance and % degradation was calculated using the following formula.

$$\%Degradation\ of\ polymer = \frac{IW - FW}{FW} \times 100$$

Where, IW- Initial weight, FW- Final weight.

2.5.4. Floating and lag time

In-vitro buoyancy and the floating lag time of the prepared nanofiber film were determined as per the method discussed by Jimenez Castellanos et al. [16]. Prepared nanofiber film of 5 cm^2 area was placed into a 1000 mL beaker containing 900 mL of SGF, maintained at 37 °C. The time taken by the film to rise to the surface of the medium was considered as buoyancy lag time and the time of which the film floats on the surface was determined as the floatation time.

2.5.5. Cytotoxicity assay

Percentage cell viability of plain drug and developed nanofiber formulations was measured against EAC cell lines. Briefly, samples in different dilutions were incubated to the experimental cells having a cell density of 3.24 × 10^4 cells. After the predefined period, the cells were treated with MTT reagents and the orange formazan produced was analyzed by taking the absorbance at 490 nm. The relative cell viability was determined against the negative control (Fresh basal medium). The cell viability of the drug-loaded scaffold and the plain drug was systematically compared [17].

$$Percentage\ cell\ viability = \frac{As - Ab}{Ac - Ab} \times 100$$

Where, As = absorbance of sample, Ac = absorbance of blank, Ab = absorbance of control.

2.5.6. Animals study and tumor induction

An animal experiment conducted in the present study was approved by the Institutional Animal Ethical Committee (IAEC) at ISF College of Pharmacy, Moga, India. The animal studies approved (ISFCP/IAEC/CPCSEA/Meeting No.24/2019/Protocol No. 406) complying all the regulations and guidelines recommend by CPCSEA (Committee for Prevention, Control and Supervision of Experimental Animals). Stomach cancer was induced in experimental animals with a dose of 1x10^7 EAC cells given by intragastric gavage.

2.5.6.1. Tumor regression study. The mean tumor regression volume was determined on the 14th and 21st days of dosing. The tumor volume was calculated using a Vernier calliper. On a predefined time, frame, tumors were removed aseptically from the animals and have been dissected perpendicularly in X and Y plain to address the largest diameter. The largest axial length was measured by 4 independent skilled technicians using a Vernier calliper. The tumor volume was determined using the following equation.

$$Volume = \frac{XY^2}{2}$$

2.5.6.2. X-ray transmission radiography. X-ray radiographic technique was used to access the gastro-retention behavior of the prepared nanofiber film. For which a separate batch containing radiocontrast media (barium sulfate) was prepared to locate the position of the nanofibers after oral administration [18]. The study involves oral administration of barium sulfate impregnated nanofiber film to fasted animals with free access to water. X-ray images of the stomach of the rats were taken at various time intervals 2, 4, 8, 12hrs after the administration using L&T Vision 100 (C-arm) X-ray machine.

2.5.6.3. Pharmacokinetics study. Pharmacokinetic profiling of prepared formulation was performed following oral administration to animals, which were kept fasting overnight with free access to water. In the present study final formulation was considered as test formulation while plain drug as control. 5-FU at a dose of 15 mg/kg body weight in the sodium carboxymethyl cellulose suspension (0.5%, w/w) was administered following the oral route using the GI catheter. On the other hand, prepared nanofiber formulation containing an equivalent dose of 5-FU was administered orally to the test group. Approx. 1.2 ml of blood samples was collected from the retroorbital site over a predefined period after oral administration. Immediately after collection, each blood sample was centrifuged at 5000×*g* for 10 min. Plasma was recovered and kept at −20 °C for further analysis. The frozen plasma sample was thawed at room temperature. The sample was further processed as per our previous method with little modification [19]. In brief, 0.5 mL of plasma sample was taken into a 5 mL centrifuge tube and 5 ml of ethyl acetate was added. The mixture was vortexed for 5 min and the layer of ethyl acetate was pipette out. Then the layer of ethyl acetate was

evaporated and 2 ml of 5 mM KH_2PO_4 was added. Then, '100 µL sample of the clear supernatant was injected onto a high-performance liquid chromatography (HPLC) system.

2.5.6.4. Histopathology. It was performed on the 21st day. For histopathology examination, local tissue including the tumor was successfully removed from animals and was then fixed in 10% neutral buffer formalin immediately after its removal and then dehydrated and embedded in paraffin. Cross-sections were made with a size of about 3–4 mm and stained with dyes (haematoxylin and eosin). The prepared samples were viewed under a microscope.

2.6. Statistical analysis

Statistical analysis of critical outcomes was analyzed using one-way ANOVA followed by Tukey's multiple composition tests. All the major outcomes were presented as mean ± SD. A P-value of less than 0.05 was assumed as a statistically significant value.

3. Results and discussion

3.1. Structural, chemical, and thermal characterization

The morphology of optimized nanofibers was determined using SEM as described in the methods. Scanning electron micrograph of plain nanofiber and 5-FU loaded nanofiber are shown in Fig 1A1 and B1 respectively. The drug-loaded nanofibers showed a larger diameter, which could be due to the incorporation of drugs in the polymeric nanofibers. SEM further suggested that Eudragit S-100 drug-loaded nanofibers showed good homogeneity, nonwoven, non-beaded smooth, and ultrafine in nature. Surface properties remain unchanged after drug loading, indicated good solvency behavior of the drug in the selected polymer mixture. Further a high density of interconnected fiber network observed in both plain and drug-loaded nanofibers could be related to higher polymer conductivity that allows random distribution of fibers. These outcomes are somewhat supported by Radzuan et al. where he concludes higher polymer conductivity increases piezoelectric pressure on nanofibers leads to the random distribution of polymeric nanofibers [20]. Moreover, the addition of drugs found to not affect porosity or fiber alignment.

The compatibility between the drug and polymer was investigated by FTIR spectra. The position of the characteristic peak in the FT-IR spectra of pure 5-FU was compared with standard. It was observed that there was no disappearance or shift in the bond position of functional groups, which interfered there is no interaction between drug and excipient. The spectra of 5-FU and drug-loaded nanofibers are presented in Fig 1A2 and B2.

DSC thermogram of 5-FU shows a sharp endothermic peak at 284.9 °C (Fig. 1 C1), which compiles with the melting point of the drug. DSC thermogram of drug loaded Eudragit S-100 nanofibers shown distinct peak at 276.9 °C as shown in Fig. 1 C2. The characteristic peak of the drug seemed to be slightly changed in nanofibers owing to the loss of the original crystalline state of the drug. A small change in glass transition temperature of 5-FU in the prepared formulation may be related to instant solidification of liquid jet, prevent the formation of stable drug crystal. Our outcomes are in alignment with the results reported by Kajdic et al., where the authors reported a significant increment in the solubility of Soluplus in polyethylene oxide nanofibers related to solid-state modulation of the drug in fiber matrix [15]. In addition, the solid-state properties of the drug also depend on the drug-polymer affinity and nature of the solvent used. In an earlier study, Illangakoon and co-workers observed significant improvement in 5-FU solubility in core-shell nanofibers comprising of Eudragit S100, attributed to self-emulsifying properties of Eudragit S100 which control the drug crystallization through hydrogen bond formation [21]. Self-emulsifying properties of Eudragit S100 is also strongly supported by the SEM inferences, wherein the smooth fiber surface suggesting good drug-polymer miscibility.

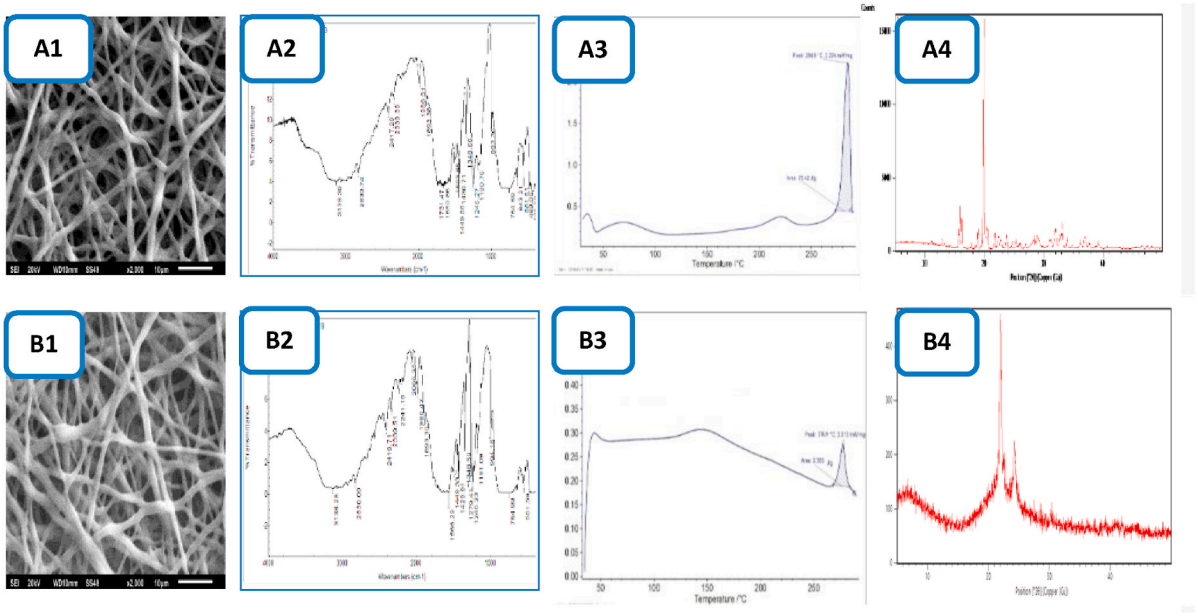

Fig. 1. Structural, chemical and physical properties of free drug and drug loaded Eudragit S100nanofibers. A1. SEM micrograph of plain nanofibers indicating the smooth surface and porous network. A2. FT-IR of plain drug (5-FU) indicating characteristic peaks used for compatibility and chemical identity of drug in the prepared formulation. A3. DSC thermogram showing the transition temperature of plain drug for understanding any changes in the physical state of drug in the formulation. A4. X-ray diffractogram of plain drug showing the major diffraction peak for analyzing any change in the physical state of drug. B1. SEM micrograph of drug loaded nanofibers suggesting a little increment in fiber diameter. B2. FT-IR Spectra of drug loaded fibers indicating the presence of drug with all major peaks intact. B3. DSC thermogram of drug loaded fibers showing a slight decrease in glass transition temperature. B4. X-ray diffractogram of drug loaded fibers showing broad peak of drug.

3.2. X-ray diffraction

X-ray diffraction patterns of 5-FU are shown in Fig. 5.4. 5-FU shows strong diffraction peaks at $2\theta = 20^{\circ}$ well supported by the literature. The characteristic sharp diffraction peaks represent the crystalline nature of the drug. X-Ray Diffraction of the plain drug shows a sharp peak at 2θ (22°), as shown in Fig. 1 D1. The XRD patterns of the fibers do not show any Bragg reflections, only the broad humps, indicating the amorphous nature of encapsulated drug in fiber matrix (Fig. 1 D2). The XRD findings are also supported by DSC and SEM outcomes.

3.3. In-vitro release

The percentage cumulative drug release from plain drug and optimized drug loaded nanofibers with time is shown in Fig. 2 A. The release pattern demonstrated the plain drug shows complete dissolution within 1hr, whereas the formulation takes approx. 12hrs for complete dissolution in the simulated gastric fluid. The in-vitro release profile of optimized formulation exhibits an initial burst release of approx. 40% within 3 h followed by a steady release may be due to larger amounts of surface-associated drug and the high surface area of fibres. Following burst release, an extended drug release was observed which is attributed to diffusion mechanism. In-vitro drug release of prepared nanofiber exhibits reproducible kinetics for predetermined period with fractional drug release values (t_{25}, t_{50} and t_{75}) after 2, 6 and 10 h, suggests approximately 25% (4 mg) of drug release within an interval of 3–4 h sufficient to maintain local tissue level of drug (500–600 μg/mL) necessary to produce desired therapeutic action. Although the polymer is insoluble at this pH, around 80% of the drug release was reached after 8hrs (Fig. 2B). These observations are ascribed to the low molecular weight of 5-FU permitting it to diffuse through pores. Our observations substantiate earlier findings by Ammar et al. where authors concluded that risperidone release primarily governed by diffusion mechanism from the floating microparticles of Eudragit S100 and hydroxypropyl methylcellulose in SGF [22]. Further the high acid solubility of the drug providing a thermodynamic impetus for this to happen. In addition, the fibers were observed to be broken at pH 1.2, providing additional escape routes for the 5-FU.

The release patterns were fitted on various kinetic models such as Zero, First, and Higuchi. The correlation coefficient of the straight line that has the highest value was used to compare between different models (Fig. 2C). The optimized formulation was best fit to the Higuchi model as the value of r^2 is highest i.e. 0.981 which indicates that formulation shows the drug release by anomalous transport (Non-Fickian). This model is widely used; when the release mechanism is not well known or when more than one type of release phenomenon could be involved. Anomalous transport means drug diffusion in the hydrated matrix and polymer relaxation.

3.4. Encapsulation efficiency

The drug encapsulation efficiency as calculated by UV analysis was found to be almost 98 ± 1.4%. The amount of drug entrapped in the fibers was found to be almost equal to the amount of drug that was added during the process of loading. Approx. 100% drug loading suggested selected formulation and process conditions best suited to produce drug-loaded fibers. Moreover, the findings suggest the developed fibers can also accommodate more drugs.

3.5. Degradation of polymer

Biodegradation of prepared nanofibers was performed using gravimetric analysis. In the studies, it was demonstrated that the degradation rate of formulation in the simulated gastric fluid in 10 days was observed. The primary degradation study under simulated gastric fluid demonstrated a slower degradation (approximate 16% of weight loss from the original weight) was observed after 10 days shown in Fig. 2B. Degradability results is a good indicator in that the developed polymeric fibers can provide better protection for the drug in the localized environment and makes them ideal drug carrier suitable for the gastro retentive drug delivery.

3.6. Tensile strength

Fig. 3Aand B represent the tensile strength of plain nanofibers and drug-loaded nanofibers respectively. Results demonstrated plain nanofibers have higher mechanical strength (170 g/cm^2) compare to drug-loaded fibers. Such outcomes may be attributed to fiber diameter. SEM results indicate plain nanofibers have smaller diameter compare to drug-loaded fibers. Smaller diameter ensures high fiber density per unit volume leading to an increase in fiber strength. Similar observations have been reported in previous literature i.e. mechanical strength of nanofibers is directly related to fiber diameter. Smaller fiber diameter not only increases in the number of fibers per unit area but also increases the degree of crystallinity and molecular orientation between nanofibers results in a considerable increment in the mechanical performance of nanofibers [23]. In contrast to this, as the fiber size increases the number of fibers per unit volume decreases proportionally, attributed to the decrease in mechanical strength.

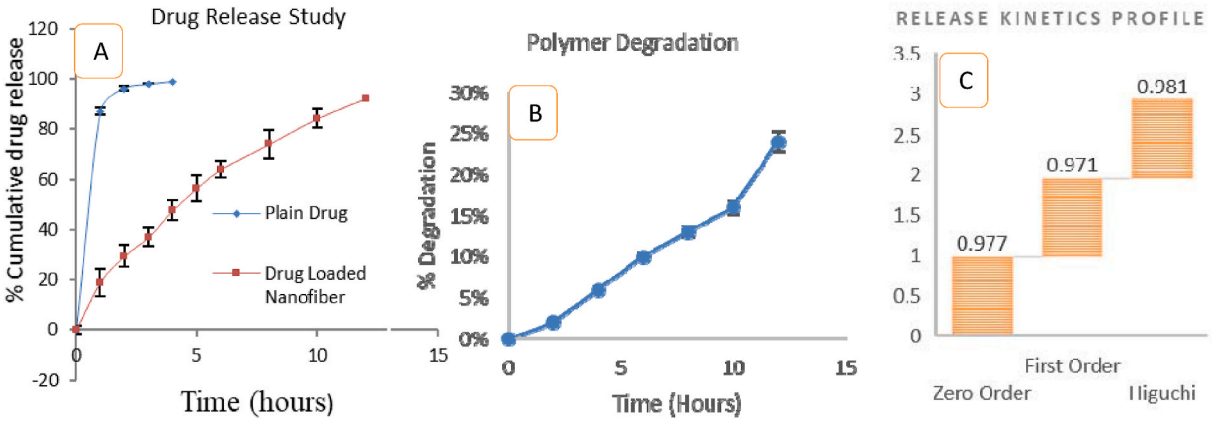

Fig. 2. Comprehensive drug release analysis. A. Schematic representation indicating comparative analysis of drug release between plain drug and drug loaded nanofibers. B. Time scale of polymer degradation in simulated gastric pH. C. Bar graph indicating the value of correlation coefficient (r2) obtained through different mathematical model for understanding the mechanism of drug release from the developed fibers.

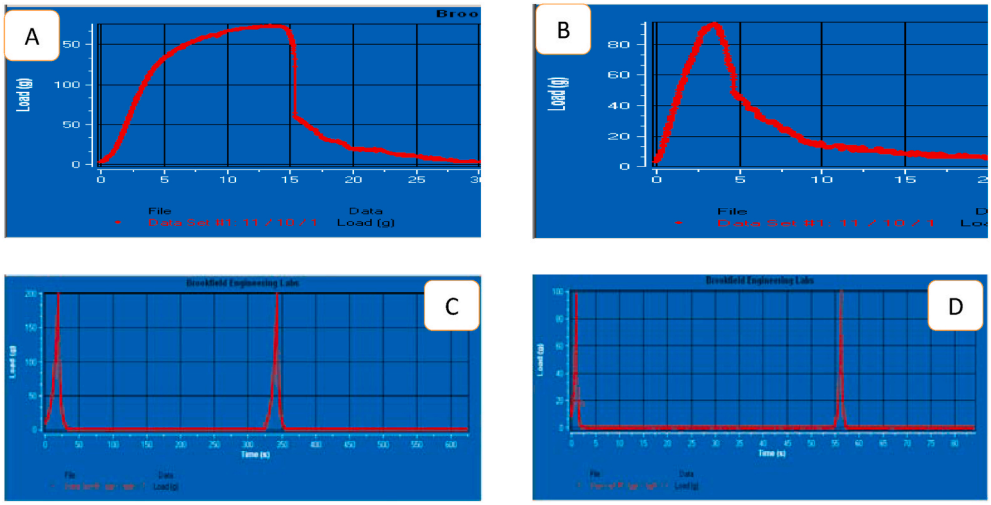

Fig. 3. Mucoadhesive and mechanical properties of prepared nanofibers analyzed by texture analyser. A. Tensile strength of plain nanofibers B. Tensile strength of drug loaded nanofibers C. Mucoadhesive detachment force of plain nanofibers D. Mucoadhesive detachment force of drug loaded nanofibers.

3.7. Mucoadhesiveness strength

Results of mucoadhesive detachment force demonstrated blank nanofibers exhibit better detachment force (200 gm/cm^2) compare to drug-loaded fibers (100 gm/cm^2) Fig. 3C and D. Experimental outcomes could be related to fiber diameter. Fibers with smaller diameter possess higher surface area leads to greater adhesive force. of nanofibers where the blank nanofibers possess smaller fiber diameter than drug-loaded nanofibers. Moreover, the number of hydrophilic groups per unit volume increases proportionally with surface area, attributed to the increase in mucoadhesive strength. In contrast to this, drug-loaded fibers with larger diameter possess a lesser number of hydrophilic groups leading to a decrease in adhesive strength.

3.8. Floating and lag time

Floating time of nanofibers at different period are shown in Fig. 4. There was no floating lag time for the drug-loaded nanofiber because the nanofiber system floated onto the surface the moment it was put into the dissolution medium and the floating time was more than 48hrs. Moreover, porosity determined by apparent densities technique shows high porosity values (78 ± 8%) and low density (0.08 ± 0.002 g/cm^3) than that of the gastric fluid, which play an important role on the floating behavior of the prepared nanofibers. Thus, it is concluded that nanofiber is a good carrier for the gastro retentive drug delivery system. These findings are in alignment with our previous result, where nanofibers due to its ultra-low-density properties show zero lag time with prolonged retention in the selected medium (Malik et al., 2015).

3.9. Cytotoxicity assay

Fig. 5 represents the dose-dependent cytotoxicity behavior of 5-FU and drug-loaded nanofiber determined after 48h of incubation against EAC cells. Results suggest drug-loaded nanofibers at different drug

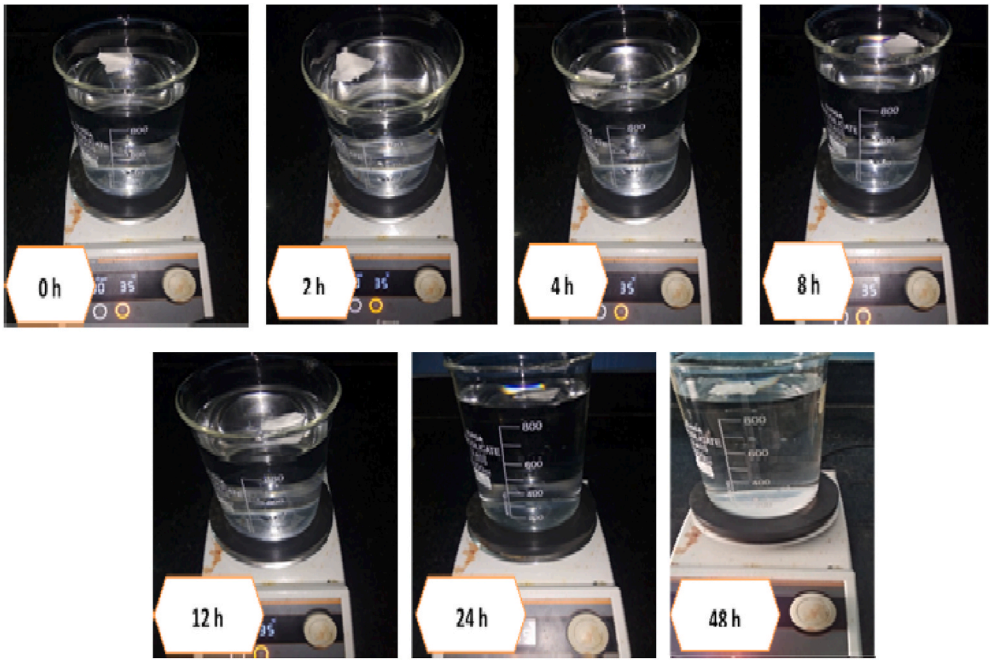

Fig. 4. In-vitro buoyancy images of nanofibers in the gastric fluid at a different time interval.

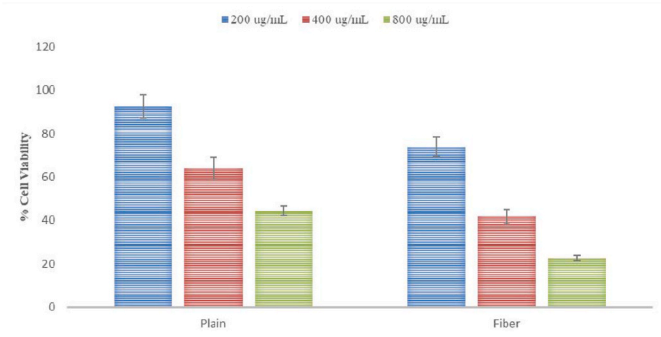

Fig. 5. Graphical presentation of comparative cell viability between plain drug and drug loaded fiber against EAC cell lines.

concentrations display enhanced cytotoxicity compared to the plain drug. Higher cytotoxicity in drug-loaded formulation could be attributed to higher drug solubility and controlled drug release behavior. Both DSC and XRD studies indicated the change in the solid-state properties of the drug in the optimized fibers. Further, there is ample evidence in favor of electrospun nanofibers for improved dissolution profiles of a wide range of drugs. In a recent study, we have found that the ocular bioavailability of fluocinolone acetonide is significantly improved when administered through PCL nanofibers, which is mainly related to the ability of electrospun fibers to improve the aqueous solubility of the drug [24]. Similarly, our experimental findings correspond strongly to previous observations, where Iqbal et al. demonstrate Paclitaxel and 5-FU loaded nanofiber exhibit higher cytotoxicity characterized by cell viability (38%) compare to plain drugs (43%) against breast cancer cells, due to increase in solubility and permeability of drugs in nanofiber [25]. Further, a burst drug release of approximately 40% within the first hour followed by an extended drug release helps to maintain a constant therapeutic drug level near the tumor microenvironment for enhanced antitumor activity. Moreover, the controlled drug release behavior of the formulation ensuring the rational approach to reduce dose-dependent cytotoxicity with higher clinical efficacy.

3.10. X-ray radiograph

Fig. 6 illustrates the X-ray radiograph indicating the intraoral position and retention period of the developed carrier after oral administration. Experimental findings demonstrate that the optimized drug-loaded nanofibers successfully retained in the stomach over an extended period i.e. up to 12hrs. The x-ray further confirms the position of fibers which is found at the upper part of the stomach ensuring the floating behavior of the carrier attributed to its ultralow density nature. Thus, nanofibers could be a promising carrier for gastro retentive drug delivery systems.

3.11. Tumor regression studies

Tumor regression studies were performed on 21st day following the administration of experimental formulations using a vernier caliper. Experimental findings suggested a significant difference in tumor volume between the drug (4.15 ± 0.38 mm^3) and formulation (2.65 ± 0.47 mm^3) treated group ($p \leq 0.05$). The tumor volume of different groups is presented in Fig 6A2. It has been observed that the plain 5-FU resulted in a decrease in the tumor volume which is due to its anticancer potential. A higher reduction in tumor volume in the case of formulation could be attributed to better dissolution profile and controlled drug release behavior from Eudragit S-100 nanofibers. Polyanionic nature of Eudragit S-100 remains undissociated in the gastric environment, allows diffusion-controlled drug release, ensures the therapeutic level of drug near the target over an extended period result in a higher decrease in tumor volume. These findings are consistent with cytotoxicity results, where the optimized formulation shows greater cytotoxicity against EAC cell lines than plain 5-FU.

3.12. Pharmacokinetics

Plasma concentration of drug at different time point was determined using a reliable HPLC method produces a linear response in the range of 0.1–10 μg/mL having a limit of 0.0029 mg/mL and correlation coefficient $r^2 = 0.999$. Fig. 6 A1 represents the plasma drug profile of the plain drug and drug-loaded nanofibers following oral administration. Results indicate a significant improvement in all pharmacokinetic parameters (C_{max}, T_{max}, and AUC) in the nanofiber group compare to the plain drug ($p \leq 0.05$). Improved pharmacokinetic profile in the nanofiber group is attributed to a better dissolution profile and controlled drug release behavior from Eudragit S-100 nanofibers. The higher C_{max} value is associated with greater systemic toxicity, but both the results of tumor regression studies and cytotoxicity assay revealed 5-FU has greater therapeutic response per dosing equivalent in the formulation. Further, the outcomes support the concepts of minimum effective therapeutic dose tends to reduce the systemic toxicity. Nanofibers produced an approximately 30% increase in AUC compared to a plain drug, which could be related to increasing in apparent drug solubility and desirable release kinetics of the prepared carrier, leads to a decrease in dose-dependent toxicity.

3.13. Histopathology

Fig. 6 B1–B4 presents the histogram of stomach tissues of different experimental groups at a magnification level of 100×. The histogram indicates a uniform pattern of tissue distribution in normal groups. On the other hand, disease control groups show structural abnormality of mucosal lining with large infiltration of inflammatory cells. Histogram of treated groups (5-FU and drug-loaded nanofibers) indicate significant improvements in the structural aspect without any evidence of inflammatory cells. However, restoration of structural barriers seems to be better in the nanofiber group characterized by distinct epithelium supported by clear connective tissue layers. Improved tissue restoration in the nanofiber group is related to the controlled drug release kinetics of prepared structure, helps in maintaining a higher local concentration of the chemotherapeutics near the tumor tissue, and minimize systemic drug toxicity.*In-vivo* retention performance of prepared nanofibers.

4. Conclusion

In the present work, a nanofiber-based gastro retentive drug delivery system comprising of the stimuli-responsive polymer was successfully prepared using the electrospinning technique. Inclusive in-vitro characterization studies indicated the developed fibers exhibits desired physical, chemical, mechanical and pharmaceutical properties for controlled and localized delivery of encapsulated chemotherapeutics. Results of cytotoxicity studies suggest drug-loaded nanofibers enhanced cytotoxicity compared to the plain drug. Further, the prepared nanofibers show improved pharmacokinetic and tissue regression profile could be related to an increase in apparent drug solubility and desirable release kinetics of the prepared carrier leads to a decrease in dose-dependent toxicity. This may help to reduce the total dose required for cancer therapy and ultimately reduce the dose-related systemic side effects which are the major goal and scope of this work. This project can open a new avenue in the treatment of stomach cancer and can be an alternative to painful intravenous therapy.

4.1. Financial & competing interests' disclosure

The authors have no relevant affiliations or financial involvement with any organization or entity with a financial interest in or financial conflict with the subject matter or materials discussed in the manuscript.

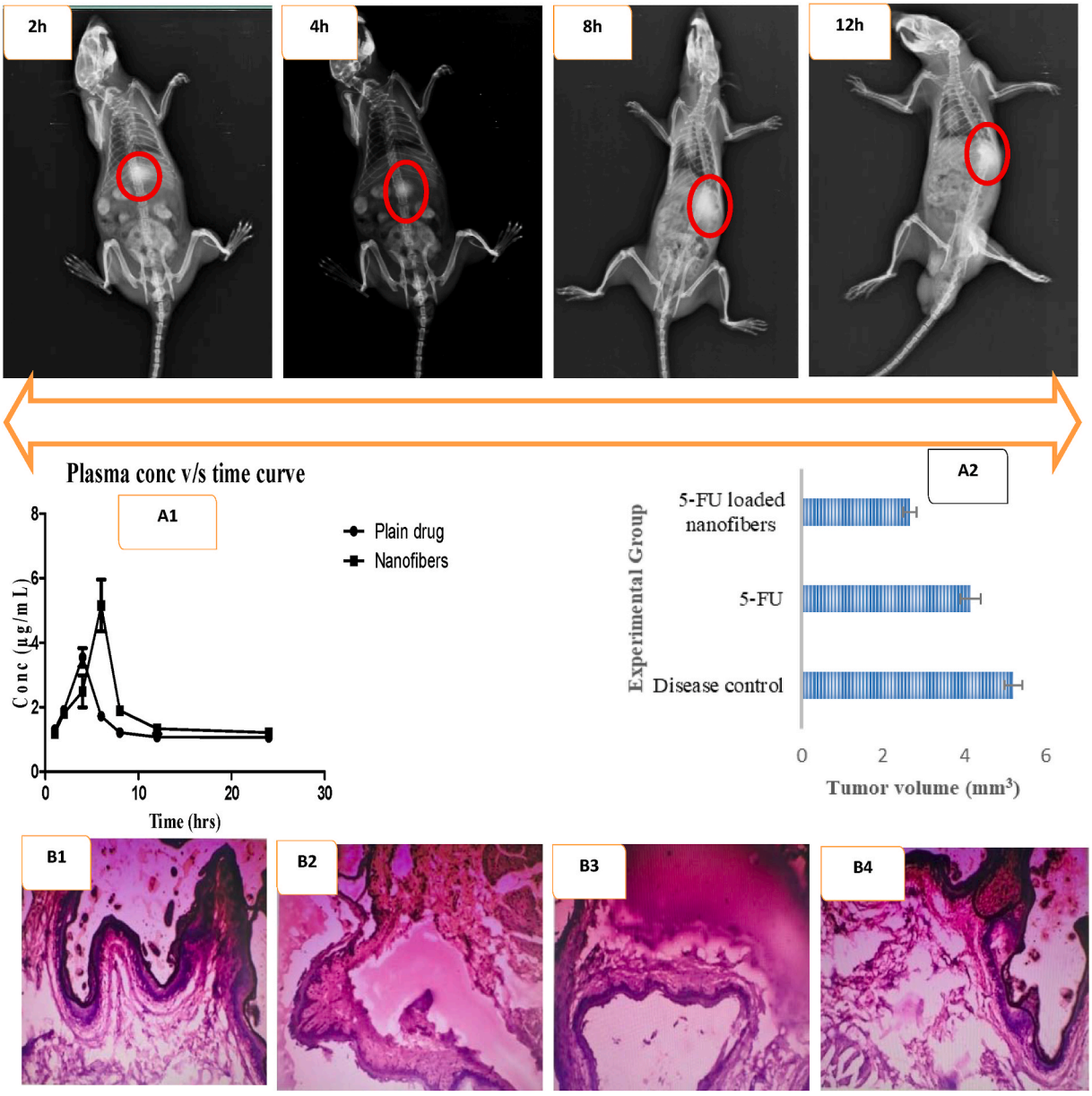

Fig. 6. In-vivo biopharmaceutical performance of 5-FU loaded nanofibers. Top row represents the gastric retention of prepared nanofibers at different time period. Bright spot in circle indicate the presence of radiocontrast material, which is impregnated in the nanofibers. Image after 12h of administration clearly suggested the presence of nanofiber in stomach. A1: Comparative analysis of pharmacokinetic profile between drug and drug loaded nanofibers indicating improved pharmacokinetics parameters of nanofibers group including Cmax, Tmax and AUC compared to plain drug. A2: Comparative analysis of tumor regression performance between different group of xenograft tumor model. Finished formulation shows maximum regression in tumor volume followed by plain drug and disease control. Stomach histopathology after 21 days of drug administration B1: Normal stomach B2: Disease control B3: Plain 5-FU B4: Drug loaded nanofibers.

This includes employment, consultancies, honoraria, stock ownership or options, expert testimony, grants or patents received or pending, or royalties. All the authors involved in this manuscript declare no conflict of interest.

Credit author statement

I am enclosing herewith a revised manuscript entitled "**Development and characterization of 5-fluorouracil nanofibrous film for the treatment of stomach cancer**" for publication in Journal of Drug Delivery Science and Technology for possible evaluation. All authors of this research paper have directly participated in the planning, execution, or analysis of this study. All the following author(s) declare that there is no conflict of interest regarding the publication of this article. I (Goutam Rath) on behalf of all the authors agree with the conditions stated below

- o All authors have participated in (a) conception and design, or analysis and interpretation of the data; (b) drafting the article or revising it critically for important intellectual content; and (c) approval of the final version.
- o This manuscript has not been submitted to, nor is under review at, another journal or other publishing venue.
- o The authors have no affiliation with any organization with a direct or indirect financial interest in the subject matter discussed in the manuscript
- o The following authors have affiliations with organizations with direct or indirect financial interest in the subject matter discussed in the manuscript:

Declaration of competing interest

All the authors declared no conflict of interest.

References

[1] J. Ferlay, I. Soerjomataram, R. Dikshit, et al., Cancer incidence and mortality worldwide: sources, methods and major patterns in GLOBOCAN 2012, Int. J. Canc. 136 (2015) E359–E386.
[2] S.-H. Kong, D.J. Park, H.-J. Lee, et al., Clinicopathologic features of asymptomatic gastric adenocarcinoma patients in Korea, Jpn. J. Clin. Oncol. 34 (2004) 1–7.
[3] S.M. Jeurnink, E.W. Steyerberg, Hof G. van 't, et al., Gastrojejunostomy versus stent placement in patients with malignant gastric outlet obstruction: a comparison in 95 patients, J. Surg. Oncol. 96 (2007) 389–396.
[4] M. Narvekar, H.Y. Xue, J.Y. Eoh, et al., Nanocarrier for poorly water-soluble anticancer drugs—barriers of translation and solutions, AAPS PharmSciTech 15 (2014) 822–833.
[5] U.K. Mandal, B. Chatterjee, F.G. Senjoti, Gastro-retentive drug delivery systems and their in vivo success: a recent update, Asian J. Pharm. Sci. 11 (2016) 575–584.
[6] A. Verma, J. Dubey, R.R. Hegde, et al., Helicobacter pylori: past, current and future treatment strategies with gastroretentive drug delivery systems, J. Drug Target. 24 (2016) 897–915.
[7] R. Malik, T. Garg, A.K. Goyal, et al., Polymeric nanofibers: targeted gastro-retentive drug delivery systems, J. Drug Target. 23 (2015) 109–124.
[8] R. Malik, T. Garg, A.K. Goyal, et al., Diacerein-Loaded novel gastroretentive nanofiber system using PLLA: development and *in vitro* characterization, Artificial Cells, Nanomed. Biotechnol. 1–9 (2015).
[9] P.R. Gibson, B. Fixa, B. Pekarkova, M. Bátovský, G. Radford-Smith, J. Tibitanzl, L. Gabalec, T.H. Florin, R. Greinwald, Comparison of the efficacy and safety of Eudragit-L-coated mesalazine tablets with ethylcellulose-coated mesalazine tablets in patients with mild to moderately active ulcerative colitis, Aliment Pharmacol. Therapeut. 23 (7) (2006 Apr) 1017–1026.
[10] S. Thakral, N.K. Thakral, D.K. Majumdar, Eudragit®: a technology evaluation, Expet Opin. Drug Deliv. 10 (1) (2013 Jan 1) 131–149.
[11] R. Cortesi, L. Ravani, E. Menegatti, E. Esposito, F. Ronconi, Eudragit® microparticles for the release of budesonide: a comparative study, Indian J. Pharmaceut. Sci. 74 (5) (2012 Sep) 415.
[12] F. Takabayashi, H. Sekiguchi, Viscous methyl cellulose solution thickens gastric mucosa and increases the number of gland mucous cells in mice, Br. J. Nutr. 110 (2013) 1195–1200.
[13] P. Rathee, M. Jain, A. Garg, A. Nanda, A. Hooda, Gastro intestinal mucoadhesive drug delivery system. A review, J. Pharm. Res. 4 (5) (2011 May), 1488-53.
[14] G.C. Rajput, F.D. Majmudar, J.K. Patel, K.N. Patel, R.S. Thakor, B.P. Patel, N. B. Rajgor, Stomach specific mucoadhesive tablets as controlled drug delivery system–A review work, Int J Pharm Biol Res 1 (2010) 30–41.
[15] H.S. Johal, T. Garg, G. Rath, et al., Advanced topical drug delivery system for the management of vaginal candidiasis, Drug Deliv. 23 (2016) 550–563.
[16] H. Singh, R. Sharma, M. Joshi, et al., Transmucosal delivery of Docetaxel by mucoadhesive polymeric nanofibers, Artificial Cells, Nanomed. Biotechnol. 43 (2015) 263–269.
[17] M. Jimenezcastellanos, H. Zia, C. Rhodes, Design and testing in vitro of a bioadhesive and floating drug delivery system for oral application, Int. J. Pharm. 105 (1994) 65–70.
[18] P. Kaur, K.J. Singh, A.K. Yadav, et al., Growth of bone like hydroxyapatite and cell viability studies on CeO2 doped CaO–P2O5–MgO–SiO2 bioceramics, Mater. Chem. Phys. 243 (2020), 122352.
[19] N.A. Mohd Radzuan, A.B. Sulong, D. Hui, et al., Electrical conductivity performance of predicted modified fibre contact model for multi-filler polymer composite, Polymers 11 (2019).
[20] S. Kajdič, Zupančič Š, R. Roškar, et al., The potential of nanofibers to increase solubility and dissolution rate of the poorly soluble and chemically unstable drug lovastatin, Int. J. Pharm. 573 (2020) 118809.
[21] U.E. Illangakoon, D.-G. Yu, B.S. Ahmad, et al., 5-Fluorouracil loaded Eudragit fibers prepared by electrospinning, Int. J. Pharm. 495 (2015) 895–902.
[22] H.O. Ammar, M.M. Ghorab, A.A. Mahmoud, et al., Formulation of risperidone in floating microparticles to alleviate its extrapyramidal side effects, Future J. Pharmaceut. Sci. 2 (2016) 43–59.
[23] S.-C. Wong, A. Baji, S. Leng, Effect of fiber diameter on tensile properties of electrospun poly(ε-caprolactone), Polymer 49 (2008) 4713–4722.
[24] J. Singla, T. Bajaj, A.K. Goyal, et al., Development of nanofibrous ocular insert for retinal delivery of fluocinolone acetonide, Curr. Eye Res. 44 (2019) 541–550.
[25] S. Iqbal, M.H. Rashid, A.S. Arbab, et al., Encapsulation of anticancer drugs (5-fluorouracil and Paclitaxel) into polycaprolactone (PCL) nanofibers and in vitro testing for sustained and targeted therapy, J. Biomed. Nanotechnol. 13 (2017) 355–366.